Structural Integrity Assessment and Large Deformation Analysis of Metallic Components

Shaowei Hu

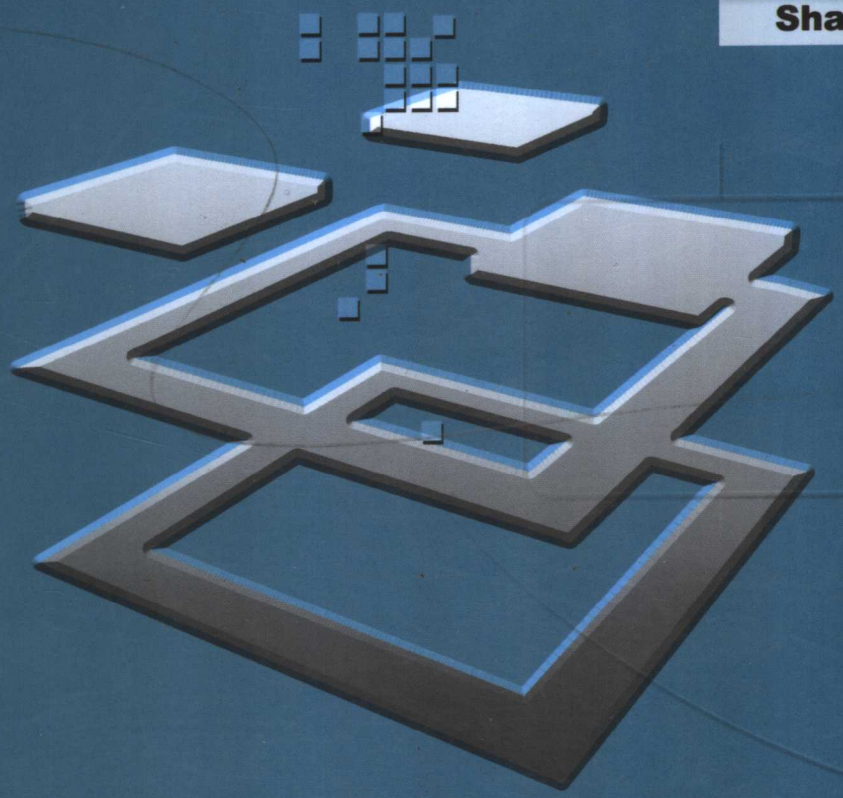

Yellow River Conservancy Press

Structural Integrity Assessment and Large Deformation Analysis of Metallic Components

Shaowei Hu

Yellow River Conservancy Press

内 容 提 要

结构完整性评估和大变形分析一直是土木、机械和力学及其航空航天领域专家学者研究的重要课题。本书是作者通过多年研究工作在结构非破坏性评估和结构大变形计算分析方面的简略总结。书中首次把有限元线法引入断裂力学，推导建立了断裂有限元线法，用于结构的完整性分析和评估。全书分为四部分：第一部分(第一、二、三、四和五章)叙述了断裂有限元线法及其在机翼开裂分析中的应用以及与一阶可靠性法相结合评估结构完整性方面的研究成果；第二部分(第六、七章)介绍了最新超声波检测结构疲劳裂缝技术以及定量非破坏性评估技术与概率可靠性方法相结合的应用情况；第三部分(第八、九、十、十一和十二章)详细提供了两种大变形理论在某发动机飞轮圆盘分析评估中的应用，给出了爆炸强度和开裂屈服的计算方法，并与其他软件进行了分析对比；第四部分(第十三章)初步分析了材料不连续屈服特性对结构失稳和破坏的影响规律。

本书可供有关科研、设计和工程单位的科技工作者参考，也可作为高等院校土木、水利、力学及其机械类专业研究生的教学参考书。

本书由南京水利科学研究院专著出版基金资助出版。

图书在版编目(CIP)数据

Structural Integrity Assessment and Large Deformation Analysis of Metallic Components (结构完整性评估和大变形分析)/胡少伟著. —郑州：黄河水利出版社，2006.1
ISBN 7-80734-014-2

Ⅰ.结… Ⅱ.胡… Ⅲ.工程结构－研究－英文
Ⅳ.TU3

中国版本图书馆 CIP 数据核字(2005)第 146964 号

出 版 社：黄河水利出版社
地址：河南省郑州市金水路 11 号　　邮政编码：450003
发行单位：黄河水利出版社
发行部电话及传真：0371—66026940　　传真：0371—66022620
E-mail：yrcp@public.zz.ha.cn
承印单位：河南省瑞光印务股份有限公司
开本：787 mm × 1 092 mm　1 / 16
印张：11.25
字数：260 千字　　印数：1—1 000
版次：2006 年 1 月第 1 版　　印次：2006 年 1 月第 1 次印刷

书号：ISBN 7-80734-014-2 / TV · 440　　定价：26.00 元

Preface

The objectives of the book were to develop a methodology for fatigue reliability and lifetime prediction of metallic aircraft components (such as wing and engine disk) within the framework of condition based maintenance. Toward this aim, a simple scheme for stress and crack analysis based on the finite element method of lines (FEMOL) was developed and combined with fatigue reliability modeling using the first order reliability method (FORM). As proof of concept, the combined techniques were applied to a test case consisting of fatigue reliability assessment of a crack emanating from a weep hole in a C141 airplane wing. A novel method of fitting a closed form mathematical expression for POD to experimental C-scan inspection data from C141 weep holes was used in the analysis.

Weep holes in C141 aircraft have been found to be locationed for the initiation of fatigue crack growth. The implementation of a neural network assisted, automated ultrasonic inspection technique from the outside of the wing was described. Toward achieving this goal of field implementation of an automated inspection technique, this work demonstrates the value of numerical simulation, laboratory studies and algorithm training with samples representing in-field variation, in-field demonstration, parametric sensitivity studies and probability of detection (POD) validation. This book discusses principal aspects of condition monitoring for structural reliability. For specificity the book focuses on the development of cracks. The techniques and instrumentation for flaw detection are discussed, and the topics include measurement models, laser based ultrasonics, neural networks and integrated microsensors. Then, the use of condition monitoring in the assessment of residual structural reliability were discussed. The topics in this book include probabilistic fatigue methods and fatigue reliability. The beneficial effect of inspections with a prescribed probability of detection on the probability of failure is demonstrated for the example of cyclic loading of a component containing an edge crack. The inspection capability for the automated procedure was found to exceed both the defined inspection requirements and the ability of inspection through viewing C-scan images.

The another objective of the book was to analyze disk structural integrity using large deformation theories. Disk structural integrity is controlled by both bulk (tensile and smooth section fatigue/crack growth) and local (notch LCF and creep) structural limits. Components must be capable of sustaining over-speed conditions, usually induced by a failure in another section of the engine without breaking. Disk fracture or burst criteria are typically set by rig tests which are time consuming and expensive. The highest temperature experienced by a disk

is in the blade attachment location where complex stress-fields and geometries must be simulated. Thus, the formulation of constitutive laws and their application in numerical simulation of plastic instability and ductile fracture in rotating disk overload failure were presented in the book. The behaviour of an elastic-plastic rotating disk is analyzed both in the context of three dimensional theory and within the framework of the plane stress approximation. For an axisymmetric disk the possibility of bifurcation into a non- axisymmetric mode is investigated. Computations are also made for the behaviour of a disk with initial imperfections either in the form of a thickness variation of in the form of material inhomogeneities. Calculated Analysis for Rotating Disk were finished using Abaqus and Ansys Software. Finally, the Role of Discontinuous Yield of Material was studied in detail. For a ductile, bored disk of uniform thickness it is found that explode occurs after the critical bifurca-velocity in the axisymmeric solution.

The methods and results presented in the book would eliminate the fuel tank entry requirement, drastically reduce weep hole and disk crack inspection costs, and reduce detection variability between technicians in making classification calls. The methods show promise for development as a standalone personal computer based system for life cycle management based on quantitative non-destructive evaluation, structural integrity and reliability assessment.

The book has been written to serve not only as a tool book for collage and university graduate students, but also as a reference book for practicing engineers and researchers as well. The book will promote the Structural Integrity Assessment and Large Deformation Analysis of Metallic Components, and it will be of great interest to civil and mechanics engineers.

In closing, the author wishes to express his sincere thanks and appreciation to the many individuals (his students, teachers, and practicing engineers) who have both directly and indirectly contributed to the content of the book. One person most deserving of special recognition is Prof. Brian Moran, who is dean of department of Civil Engineering, Robert R. McCormick School of Engineering and Applied Science, Northwestern University, USA. It is under his supervisions and helps from February, 2000 to August, 2003 in Northwestern University that the author finished above research contents and projects.

Finally, the book is sponsored by Nanjing hydraulic Research Institute publish foundations.

Shaowei Hu
August 18, 2005

List of symbols

Symbol	Definition
A	constant in material strain-hardening relation
a , b	elastic-plastic boundary; current inner and outer radii of disk
a_0 , b_0	initial inner and outer radii of disk
D	variable coefficient relating stress and strain
E	variable modulus of elasticity; modulus of elasticity
E_r , e_θ, e_z	engineering strains in radial, circumferential and axial directions
n	constant in strain-hardening relation
r , θ, z	radial, tangential and axial directions, respectively
r_0	initial radius to a point (reference state)
r	elastic-plastic boundary radius to a point
t	current thickness of disk of radius
t_0	initial uniform thickness of disk
u	radial displacement
Y	yield strength stress of material
α	radius ratio in undeformed state , = b_0 / a_0
ρ	mass density
ξ	r_0 / a_0 in undeformed state
ω	angular velocity
σ_y	yield strength stress of material
ν	poisson's ratio
σ_r , σ_θ , σ_z	radial, tangential and axial stresses, respectively
τ_r , τ_θ , τ_z	nominal stress in radial, circumferential and axial direction
ε_r , ε_θ , ε_z	radial, tangential and axial strains, respectively
η	a / b radius of elastic-plastic interface/total radius
Ω	$\frac{\rho\omega^2 b^2}{\sigma_0}$ speed factor
μ	u / b displacement ratio

(other symbols in book have been given clear indications in relative chapters)

CONTENTS

Chapter 1 Finite Element Method of Lines (FEMOL)

1.1 Introduction

Many aircrafts in both civilian and military fleets are becoming old. It is expected that many of the systems that were built twenty or thirty years ago will not be replaced in the near future by next generation structures and equipment. Consequently, these aging systems will have to be kept in service for the next decade or more. This is feasible provided adequate measures are taken to prevent poor performance, inadequate safety and increasingly expensive maintenance. This need for extended life expectancy does raise substantial technical challenges, however. In the following, our response to these challenges is summarized and the key outcomes of the research are delineated.

In the area of fatigue reliability, the key challenge is the assessment of the effect of (possibly undetected) flaws and defects on the structural integrity of a safety critical component. To meet this challenge, new computational tools are required in the areas of risk assessment and in simulation of fatigue crack propagation. Fatigue reliability (or risk assessment) methods provide an estimate (or probability) of failure over the course of the expected lifetime of the component. The effects of NDE inspections can be taken into account. Fatigue crack propagation is inherently a random process and probabilistic fracture mechanics methods are usually required. Typically, randomness in fatigue crack propagation parameters and in the detection of cracks is accounted for. The estimate of failure probability is obtained by carrying out fatigue crack propagation simulations for different values of the random variables.

We present a new method for stress and crack analysis based on the finite element method of lines (FEMOL). The method retains many of the advantages of the finite element method while also benefiting from powerful differential equation solvers. Key features of the method the ease of mesh generation and the additional accuracy associated with the semi-analytic nature of the method. The FEMOL was developed for two and three-dimensional fracture mechanics and combined with fatigue reliability modeling using the first order reliability method (FORM). A stress analysis of a simplified C141 weep hole configuration was carried out to obtain an expression for stress intensity factors. A novel method of fitting a closed form mathematical expression for POD to experimental C-scan data from C141 weep holes was used in the analysis. The FEMOL and FORM methods are then combined to compute fatigue reliability for the weep hole configuration. The method shows

promise for development as a standalone personal computer based system for structural integrity and reliability assessment.

The principal accomplishments of the program are summarized below:

(1) Developed FEMOL for two- and three-dimensional fracture mechanics including a singularity subtraction technique for modeling crack-tip fields.

(2) Developed a procedure for fitting a mathematical expression for POD to experimental data (from C141 weep holes).

(3) Combined FEMOL and FORM for assessment of fatigue reliability in C141 weep hole configuration.

First, the finite element method of lines is introduced. In the method, the governing partial differential equations, defined on arbitrary domains, are semi-discretized, by finite element techniques via variational principles (or Galerkin weak forms) into a system of ordinary differential equations (ODEs) defined on discrete mesh lines (straight or curved), and then the resulting ODE system, at the present stage of the method, is solved directly by using a standard state-of-the-art ODE solver (COLSYS Software) [2]. A key feature of the method is that the approximation is continuous in one direction and discretized in a finite element fashion in the remaining direction(s). It is the continuity of the approximation in one (local) coordinate direction which gives rise to the system of ordinary differential equations. These ODEs can be solved using powerful and freely available solvers (we use COLSYS). Due to efficient in-built adaptively techniques, these solvers essentially preserve the analytical character of the method in the continuous coordinate direction. In the following, the FEMOL is described for a model two-dimensional problem. A brief description of the implementation in three-dimensions is also given. The implementation of FEMOL for linear elastic crack problems, including the singularity subtraction technique, is discussed in next chapter.

1.2 Model Boundary Value Problem

To illustrate the finite element method of lines (FEMOL) and to make connection with standard finite element methods, we consider a model two-dimensional boundary value problem involving a poisson equation (which governs, anti-plane or Mode Ⅲ crack problems, for example). The boundary value problem is specified as:

$$\begin{aligned} -\mu\nabla^2 u &= f(x,y) \quad \text{in} \quad \Omega \\ u &= u_1(x,y) \quad \text{on} \quad \Gamma_D \\ \frac{\partial u}{\partial n} &= q_1(x,y) \quad \text{on} \quad \Gamma_N \end{aligned} \tag{1-1}$$

where u is the displacement field, Ω is the domain and Γ_D and Γ_N are the Dirichlet (essential) and Neumann (natural) boundaries, respectively.

1.3 Domain Partition

In the FEMOL, the domain Ω is first partitioned into a set of elements. For illustrative purposes, we use quadrilateral type elements here (polynomial degree p=2). The element shapes depend on the element mapping functions. In general, all four edges of an element may be curved, which makes for convenient and flexible modeling of arbitrary domains. As an example, Fig. 1-1 shows a possible FEMOL mesh for an irregular 2D domain, in which <1>, <2>, ··· denote element numbers; L_1, L_2, ··· denote global mesh line numbers and 1,2,3, ··· denote global end-node numbers.

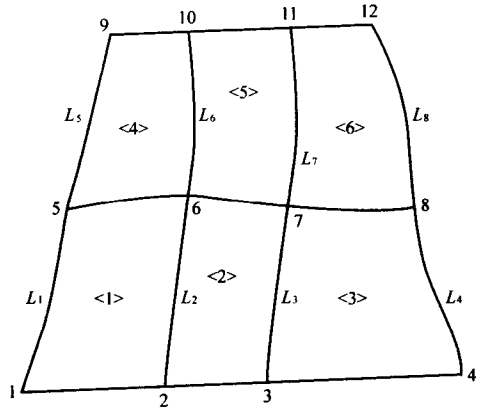

Fig.1-1 A possible FEMOL mesh

1.4 Element Mapping

Fig. 1-2 shows a typical quadratic element mapping in FEMOL from the local (or parent element) space (ξ, η) to the global (or physical) space (x, y). Element mappings of degree p (p=1,3 for linear and cubic element respectively) are treated similarly.

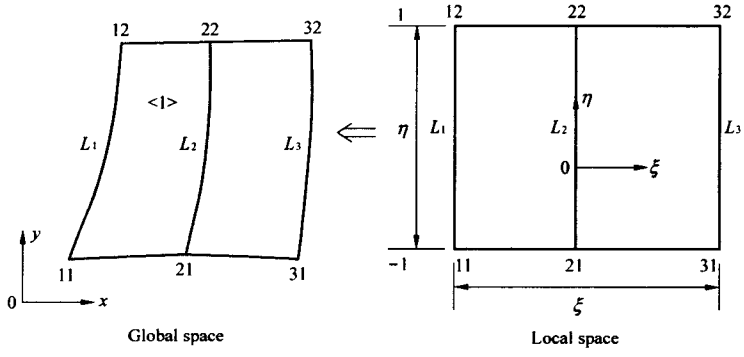

Fig.1-2 A quadratic element mapping

The curves defined by

$$\xi = \xi_i = -1 + 2(i-1)/p \tag{1-2}$$

are called the element nodal lines and the i^{th} nodal line is denoted by L_i. The two boundary curves defined by

$$\eta = \eta_j = -1 + 2(j-1) \quad j = 1,2 \tag{1-3}$$

are called the element end-sides and the j^{th} end-side is denoted by S_j. The intersection of L_i and S_j defined by

$$(\xi_i, \eta_j) = L_i \cap S_j \tag{1-4}$$

is called node ij of an element and is denoted by η_{ij}.

The element mapping is constructed in two steps: the nodal line mapping and the interpolation to the nodal lines:

Step 1: Nodal line mapping

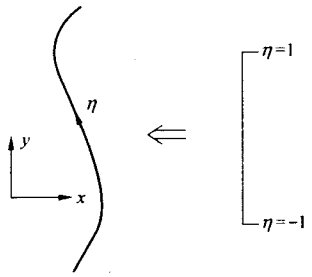

Fig.1-3 Line element mapping

The first step is to map the curved nodal lines in (x, y) space to a standard straight line segment in the parameter η from -1 to 1, so that a typical nodal line L_i is expressed parametrically as

$$x = x_i(\eta) \qquad y = y_i(\eta) \quad -1 \leqslant \eta \leqslant 1 \tag{1-5}$$

If the shape of a nodal line is relatively simple, a low degree polynomial may give a reasonable approximation. A more general approach, used here, is to divide the curved nodal line L_i into p segments with end-points (x_{ik}, y_{ik})($k = 1, 2, \cdots, p+1$). Lagrange interpolating polynomials of degree p are then used to approximate the curved nodal line as

$$x_i(\eta) = \sum_{k=1}^{p+1} N_k(\eta) x_{ik}, \quad y_i(\eta) = \sum_{k=1}^{p+1} N_k(\eta) y_{ik} \tag{1-6}$$

Particular examples are:

$$p = 1: N_1(\eta) = \frac{1}{2}(1-\eta), N_2(\eta) = \frac{1}{2}(1+\eta)$$

$$p = 2: N_1(\eta) = \frac{1}{2}(\eta^2 - \eta), \quad N_2(\eta) = 1 - \eta^2, \quad N_3(\eta) = \frac{1}{2}(\eta^2 + \eta) \tag{1-7}$$

$$p = 3: \quad N_1(\eta) = \frac{1}{16}(1-\eta)(9\eta^2 - 1), \quad N_2(\eta) = \frac{9}{10}(\eta^2 - 1)(3\eta - 1)$$
$$N_3(\eta) = -\frac{9}{10}(\eta^2 - 1)(3\eta + 1), \quad N_4(\eta) = \frac{1}{16}(1+\eta)(9\eta^2 - 1)$$

Step 2: Interpolation to nodal lines

With the nodal line mapping accomplished, the element mapping can be readily completed by using Lagrange interpolation in the ξ direction in local space, i.e.,

$$x = \sum_{i=1}^{p_1+1} N_i(\xi) x_i(\eta), \quad y = \sum_{i=1}^{p_1+1} N_i(\xi) y_i(\eta) \tag{1-8}$$

Jacobians

From the element mapping relation (2-8), we have

$$\begin{Bmatrix} \frac{\partial}{\partial \xi} \\ \frac{\partial}{\partial \eta} \end{Bmatrix} = |J| \begin{Bmatrix} \frac{\partial}{\partial x} \\ \frac{\partial}{\partial y} \end{Bmatrix} \tag{1-9}$$

Where the Jacobian matrix $[J]$ of the coordinate transformation takes the form

$$[J] = \begin{bmatrix} x_\xi & y_\xi \\ x_\eta & y_\eta \end{bmatrix} \tag{1-10}$$

and the determinant of $[J]$ given as

$$J = x_\xi y_\eta - x_\eta y_\xi \tag{1-11}$$

In the above, subscripts denote partial differentiation with respect to the indicated local coordinate. For a standard element mapping, J is required to be positive.

1.5 Trial Functions

A key step in the FEMOL is to approximate the trial function u on an element by shape functions in the ξ direction, and to leave it continuous in the η -direction. A common and convenient choice for the shape functions is the lagrange interpolating polynomials of degree p defined. It is useful to write the interpolation in matrix form:

$$u = [N]\{d\}^e \tag{1-12}$$

where

$$[N] = [N_1(\xi) \quad N_2(\xi) \quad \cdots \quad N_{p+1}(\xi)], \quad \{d\} = \{d_1(\eta) \quad d_2(\eta) \quad \cdots \quad d_{p+1}(\eta)\}^{\mathrm{T}}$$

We call $[N]$ the shape function matrix and $\{d\}^e$ the element nodal line displacement vector.

1.6 Global Energy Functional and Variational Equations

The energy functional corresponding to the model problem is given by

$$\prod(u) = \frac{1}{2} \iint_Q [(\frac{\partial u}{\partial x})^2 + (\frac{\partial u}{\partial y})^2] \mathrm{d}A - \iint_Q u f_1 \mathrm{d}A - \int_{\Gamma_N} u q_1 \mathrm{d}s \tag{1-13}$$

Continuity across common nodal lines is achieved in the element assembly procedure in a similar fashion to that in FEM. The treatment of the continuity across common element end-sides and of the essential boundary conditions will be postponed until after the system of ordinary differential equations are developed. This allows for a standard element assembly procedure which leads to the following semi-discrete global energy functional (using (1-12) in (1-13)).

$$\prod(\{d\}^e) = \frac{1}{2}\int_{-1}^{1}\{\{d'\}^T[A]\{d'\} + 2\{d'\}^T[B]\{d\} + \{d\}^T[C]\{d\}\}\,d\eta$$
$$- \int_{-1}^{1}\{d\}^T\{F\}\,d\eta - \sum_{j=1}^{2}\{d(\eta_j)\}^T\{p_j\} \tag{1-14}$$

where a prime denotes differentiation with respect to the $\tilde{\eta}$ coordinate.

The global vectors and matrices are formed by assembling the corresponding local ones. By assembling the element functional variations and then setting the first variation of the global functional to zero, i.e., $\delta\prod\{d\} = 0$, we arrive at the global variational or virtual work equation:

$$\delta\prod(\{d\}) = -\int_{-1}^{1}\{\delta d\}^T([A]\{d''\} + [G]\{d'\} + [H]\{d\} + \{F\})\,d\eta +$$
$$\sum_{j=1}^{2}\eta_j\{\delta\, d(\eta_j)\}^T(\{Q_j\} - \eta_j\{p_j\}^e) = 0 \tag{1-15}$$

It follows from the arbitrariness of $\{\delta d\}$ on (–1, 1) that

$$[A]\{d''\} + [G]\{d'\} + [H]\{d\} + \{F\} = \{0\} \qquad (-1 < \eta < 1) \tag{1-16}$$

where

$$[A] = \int_{-1}^{1} a(\xi,\eta)[N][N]\,d\xi \qquad a(\xi,\eta) = \mu[(x_\xi)^2 + (y_\xi)^2]/J$$
$$[B] = \int_{-1}^{1} b(\xi,\eta)[N]^T[N']\,d\xi \qquad b(\xi,\eta) = -\mu(x_\xi x_\eta + y_\xi y_\eta)/J$$
$$[C] = \int_{-1}^{1} c(\xi,\eta)[N']^T[N]\,d\xi \qquad c(\xi,\eta) = \mu[(x_\eta)^2 + (y_\eta)^2]/J$$
$$[G] = [A'] + [B] - [B]^T \qquad [H] = [B'] - [C]$$
$$\{F\} = \{F_A\} + \{F_L\} \qquad \{F_A\} = \int_{-1}^{1}[N]^T fJ\,d\xi$$

$$\{F_L\} = \left\{J_{L_1}q_{L_1}, 0, \cdots, 0, J_{L_{p+1}}q_{L_{p+1}}\right\} \tag{1-17}$$

Note that the load array $\{F\}$ consists of two terms, an area loading term $\{F_A\}$ (body force) and a line loading term $\{F_L\}$ (flux or traction).

The system of Equ. (1-16) is a set of second-order ordinary differential equations. This system of equations is solved using COLSYS (a freely available ODE solver) in conjunction with appropriate boundary conditions at the end points of nodal lines on the essential (Dirichlet) and natural (Neumann) boundaries. The variable coefficient matrix $[A]$ is symmetric, positive-definite, and generally of relatively small size. For a given value of η, it may be inverted numerically using efficient inversion routines.

REMARK: Because the system of ODEs is defined in terms of the local coordinate η and the ODE solver COLSYS only accepts separated boundary conditions, we always map common element end-sides to the same η -coordinate to avoid non-separated boundary conditions in the formulation.

1.7 Implementation of ODE Solver

Recall that the FEMOL gives rise to the system of ODEs (1-16), re-written here for convenience

$$[A]\{d''\}+[G]\{d'\}+[H]\{d\}+[F]=\{0\} \qquad (-1<\eta<1) \tag{1-18}$$

To illustrate the development of the coefficient matrices in the ODE system, we use linear interpolation to the nodal lines ($p=1$) and therefore

$$N_1(\eta)=\frac{1}{2}(1-\eta) \qquad N_2(\eta)=\frac{1}{2}(1+\eta) \tag{1-19}$$

The coordinates of the nodal lines are given by

$$x_i(\eta)=-\frac{n-(i-1)}{n}a \quad (i=1,2,\cdots,2n) \qquad y_i(\eta)=b\eta$$

$$x_{i+1}(\eta)=-\frac{n-i}{n}a \quad (i=1,2,\cdots,2n) \qquad y_{i+1}(\eta)=b\eta \tag{1-20}$$

where a, b are the intervals in the x and y directions respectively. Interpolation to the nodal lines is written as

$$x=\sum_{i=1}^{2}N_i(\xi)x_i(\eta) \qquad y=\sum_{i=1}^{2}N_i(\xi)y_i(\eta) \tag{1-21}$$

In element i ($i=1,2,\cdots,2n$), therefore

$$x=\frac{1}{2}(1-\xi)x_i(\eta)+\frac{1}{2}(1+\xi)x_{i+1}(\eta)=\frac{-a}{2n}[2n-2i+1-\xi]$$

$$y=\frac{1}{2}(1-\xi)y_1(\eta)+\frac{1}{2}(1+\xi)y_2(\eta)=b\eta \tag{1-22}$$

The determinant of the Jacobian matrix is

$$|J|=x_\xi y_\eta-x_\eta y_\xi=\frac{a}{2n}b \tag{1-23}$$

On an element, the displacement is

$$u=[N]\{d\} \tag{1-24}$$

where $[N]=[N_1(\xi) \quad N_2(\xi)]$, $\{d\}=\{d_1(\eta) \ d_2(\eta)\}^{\mathrm{T}}$.

Using the definitions (2-17), the coefficient matrices of Equ. (1-18) can be expressed for each nodal line as

$$[A]=\int_{-1}^{1}\alpha(\xi,\eta)[N]^{\mathrm{T}}[N]\mathrm{d}\xi=\frac{\mu a}{2nb}\begin{bmatrix}(1-\eta)^2 & 1-\eta^2\\ 1-\eta^2 & (1+\eta)^2\end{bmatrix}$$

$$[G]=[A']+[B]-[B]^{\mathrm{T}}, \qquad [G]=\frac{\mu a}{2nb}\begin{bmatrix}-2(1-\eta) & -2\eta\\ -2\eta & 2(1+\eta)\end{bmatrix}$$

$$[H]=[B']-[C]=-[C]=-\int_{-1}^{1}c(\xi,\eta)[N']^{\mathrm{T}}[N']\mathrm{d}\xi=-2\frac{nb}{a}\begin{bmatrix}1&-1\\-1&1\end{bmatrix}$$

$$\{F\}=\{F_A\}+\{F_L\},\quad \{F_A\}=\int_{-1}^{1}[N]^{\mathrm{T}}fJ\,\mathrm{d}\xi,\quad \{F_L\}=\{J_{L_1}q_{L_1}\quad J_{L_2}q_{L_2}\}^{\mathrm{T}}\qquad (1\text{-}25)$$

Assembling the coefficient matrices above for all nodal lines (i=1,2,⋯,2n), we get the overall system of ODEs for the problem:

$$[A]=\frac{\mu a}{2nb}\times\begin{bmatrix}(1-\eta)^2 & 1-\eta^2 & 0 & 0 & 0 & 0 & 0 & 0\\ 1-\eta^2 & (1+\eta)^2+(1-\eta)^2 & 1-\eta^2 & 0 & 0 & 0 & 0 & 0\\ 0 & 1-\eta^2 & (1+\eta)^2+(1-\eta)^2 & 1-\eta^2 & & 0 & 0 & 0\\ 0 & 0 & 1-\eta^2 & (1+\eta)^2+(1-\eta)^2 & & & & 0\\ 0 & 0 & 0 & 1-\eta^2 & & & & 0\\ \vdots & \vdots & \vdots & \vdots & \vdots & \vdots & \vdots & \vdots\\ 0 & 0 & 0 & 0 & 0 & 0 & (1+\eta)^2+(1-\eta)^2 & 1-\eta^2\\ 0 & 0 & 0 & 0 & 0 & 0 & 1-\eta^2 & (1+\eta)^2\end{bmatrix}$$

$$[G]=\frac{\mu a}{nb}\times\begin{bmatrix}\eta-1 & -\eta & 0 & 0 & 0 & \cdots & 0 & 0\\ -\eta & 2\eta & -\eta & 0 & 0 & \cdots & 0 & 0\\ 0 & -\eta & 2\eta & -\eta & 0 & \cdots & 0 & 0\\ 0 & & -\eta & 2\eta & -\eta & \cdots & 0 & 0\\ \vdots & \vdots & \vdots & \vdots & \vdots & & \vdots & \vdots\\ 0 & 0 & 0 & 0 & 0 & \cdots & 0 & 0\\ 0 & 0 & 0 & 0 & 0 & \cdots & 2\eta & -\eta\\ 0 & 0 & 0 & 0 & 0 & \cdots & -\eta & 1+\eta\end{bmatrix}$$

$$[H]=-2\mu\frac{nb}{a}\begin{bmatrix}1 & -1 & 0 & 0 & 0 & \cdots & 0 & 0\\ -1 & 2 & -1 & 0 & 0 & \cdots & 0 & 0\\ 0 & -1 & 2 & -1 & & \cdots & & 0\\ 0 & 0 & -1 & 2 & & \cdots & & 0\\ 0 & 0 & 0 & -1 & & \cdots & & 0\\ \vdots & \vdots & \vdots & \vdots & \vdots & & \vdots & \vdots\\ 0 & 0 & 0 & 0 & 0 & \cdots & 2 & -1\\ 0 & 0 & 0 & 0 & 0 & \cdots & -1 & (1+\eta)^2\end{bmatrix}$$

$$F=\{F_1\quad F_2\quad F_3\quad F_4\quad \cdots\quad F_{2n-1}\quad F_{2n}\quad F_{2n+1}\}^{\mathrm{T}}\qquad (1\text{-}26)$$

The system of ODEs is then solved using modern ODE solvers (such as COLSYS) called from the FEMOL code.

References

[1] Hu Shaowei, Brian Moran. The finite element of lines in fracture mechanics, Acta Mechanica Sinica, 2005.8.

[2] Yuan, S. The finite element method of lines: theory and applications, Science Press, Beijing (1994).

[3] Williams, M. L. "Stress singularities resulting from various boundary conditions in angular